

# X-ray spectral diagnostics of the immediate environment of GRB 991216

David R. Ballantyne<sup>1</sup>, Enrico Ramirez-Ruiz<sup>1</sup>, Davide Lazzati<sup>1</sup> and Luigi Piro<sup>2</sup>

<sup>1</sup> Institute of Astronomy, University of Cambridge, Madingley Road, CB3 0HA Cambridge, England  
e-mail: drb, enrico, lazzati@ast.cam.ac.uk

<sup>2</sup> Istituto di Astrofisica Spaziale, CNR, Via del Fosso del Cavaliere 100, 00133 Roma, Italy  
e-mail: piro@ias.rm.cnr.it

**Abstract.** The recent report of iron line features in the afterglow of the gamma-ray burst (GRB) 991216 has important implications for the properties of the radiating material and hence the nature of the immediate burst environment. We argue that the putative strong Fe emission line can be attributed to the reflected emission from Thomson-thick matter which is illuminated by a power-law continuum. The ionization parameter of the material (i.e., the flux to density ratio) is around  $10^3$ , resulting in a Fe  $K\alpha$  line from He-like iron. A supersolar abundance of iron is not required by the data. Interestingly, the ionizing continuum must be harder than the observed one. We interpret this as due to the fact that the observed continuum is dominated by the standard blast wave emission, while the line is produced by reprocessing material located at much smaller radii.

**Key words.** Gamma rays: bursts — X-rays: general — Radiation mechanisms: non-thermal — Line: formation

## 1. Introduction

The detection of iron emission features in the X-ray spectra of several  $\gamma$ -ray burst (GRB) afterglows (GRB 970508: Piro et al. 1999; GRB 970228: Yoshida et al. 2001; GRB 991216: Piro et al. 2000; GRB 000214: Antonelli et al. 2000) is of great importance to the understanding of the nature of the burst emission and particularly the burst progenitor (e.g., Mészáros & Rees 1998; Lazzati et al. 1999; Böttcher & Fryer 2001). All the lines have been detected roughly one day after the burst explosion due to instrumental limitations (the line may have been there at earlier times, but the afterglow was not yet observed), with an equivalent width (EW) of the order of 1 keV and a luminosity  $L_{\text{Fe}} \approx 10^{44}$  erg s<sup>-1</sup>.

The large EW inferred from the X-ray features favour models in which the line is produced by reflection from a highly ionized surface, rather than transmission. Several different emission mechanisms and geometries have been proposed to account for the line emission, all of which fall mainly into one of two categories: *geometry* dominated (GD) models or *engine* dominated (ED) models. Both classes associate the scattering medium with debris from a stellar collapse. In the GD models, the X-rays from the burst and early afterglow emission illuminate a mass  $M_{\text{Fe}} > 0.06M_{\odot}$  of iron material at a distance of about  $10^{16}$  cm from the burst location (Lazzati et al. 1999; Vietri

et al. 2001; see also Lazzati et al. 2001). This material may be associated with the remnant of a supernova that occurred days to months before the burst (Vietri & Stella 1998). Alternatively, in the ED models, the line emission can be attributed to the interaction of a long lasting outflow from the central engine with the progenitor stellar envelope at distances  $R \leq 10^{13}$  cm (Rees & Mészáros 2000; Mészáros & Rees 2001; Böttcher & Fryer 2001). In this case, only a small mass of Fe is required and there is no need for a pre-ejected supernova shell (i.e., the line can be explained if the burst and the star explode simultaneously; see Woosley 1993).

There are several ways in which these two models can be distinguished. First, the line produced by a compact reprocessor will show a higher degree of variability. It is likely that in any ED scenario the line intensity will decrease with time, mirroring the decay of energy input. Due to geometrical time dilution of the line photons, it is hard for any GD model to produce line variability on a time scale shorter than  $t_{\text{var}} < R/c \approx 1$  d. Unfortunately, the detected lines were too weak to allow for a proper variability analysis, and no firm conclusion could be made (while a hint of non-variability was derived in GRB 000214 [Antonelli et al. 2000], the line in GRB 970508 seemed to disappear before the end of the observation [Piro et al. 1999]). Secondly, different ionization parameters  $\xi \equiv L_X/(n_H R^2)$  are expected, with  $\xi \approx 10^3$  for ED models and  $\xi \approx 10^5$  for GD models. This would

suggest that ED models may produce a more luminous line (see Ballantyne & Ramirez-Ruiz 2001), but smaller ionization parameters can be predicted even for the GD models if, for example, the emitting material is clumped or the off-axis burst emission is less intense than the one we receive. The equivalent widths of the lines may also be very useful. In the ED models it is impossible to avoid seeing the ionizing continuum together with the reflected component, while it is natural in GD models to see only the reflected component. This implies (Ballantyne, Fabian & Ross 2002) that a line with  $EW > 800$  eV can be produced only by GD models irrespective of the iron abundance. Finally, broad-band X-ray spectroscopy could help settle this question. This is because in the ED case, the line should be due to material newly synthesized by the exploding star (which is mostly nickel rather than iron; see Woosley & Weaver 1995), while in the GD case, the star exploded several months before the GRB and the nickel has had time to decay into iron. It is, however, possible for nickel to be bypassed due to high neutronization (where the iron is directly synthesized by the exploding star), or by the iron being dragged out from the stellar core by the expanding fireball.

Measurements of the strength and shape of the reflection spectrum can yield the geometry, velocity, density and abundances of the scattering medium. In this paper, we attempt to fit detailed models of such reflection spectra, computed with the method described by Ross & Fabian (1993), to the X-ray afterglow of GRB 991216. This will allow, for the first time, a self-consistent determination of both the Fe  $K\alpha$  line and the continuum in a X-ray afterglow of a GRB. A description of the data and the fitting results are presented in §2. In §3 we briefly discuss the general constraints that arose from the fits in the context of both GD and ED models.

## 2. Data analysis

The most significant detection of a X-ray iron line-like feature was obtained by *Chandra* following the burst GRB 991216. The observation lasted 3.4 hours and began  $\approx 37$  hours after the initial burst explosion. The afterglow was detected with both the Advanced CCD Imaging Spectrometer (in spectroscopic mode; ACIS-S) and with the High Energy Transmission Gratings (HETG). The presence of a possible Fe  $K\alpha$  line in these data was discussed by Piro et al. (2000), who used the ACIS-S spectrum to estimate the continuum and the higher resolution gratings spectrum to measure the line properties. In this section we simultaneously fit the GRB 991216 data from both detectors with the constant density Compton reflection models of Ross & Fabian (1993) (see also Ross, Fabian & Young 1999).

Following Piro et al. (2000), the ACIS-S data between 0.4 and 8 keV (observer's frame) were grouped to have a minimum of 20 counts per bin, while counts between 1 and 6.2 keV from both the high-energy and medium-energy gratings were combined to obtain a final HETG spectrum

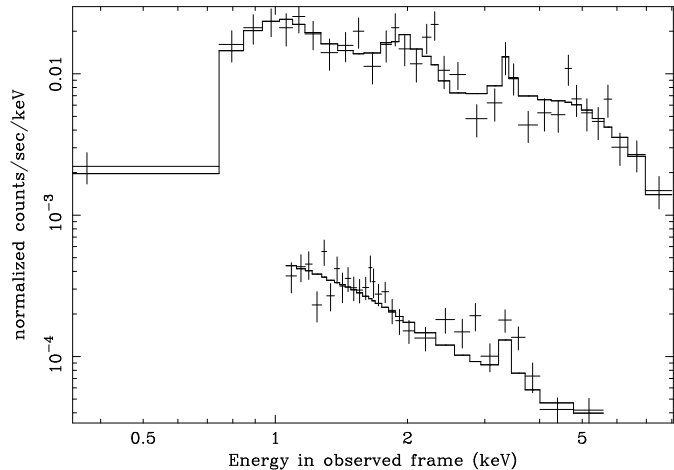


**Fig. 1.** ACIS-S (top) and HETG (bottom) count spectra of the X-ray afterglow of GRB 991216. The number of counts in the two instruments are comparable, but the influence of the effective area has been removed from the HETG data, so it is shown with a smaller normalized count rate than the ACIS-S spectrum. The best fit Compton reflection model (#9; see Table 1) convolved with the instrumental resolution is shown as solid lines for both spectra.

with 17 counts per bin (see Figure 1). The slight underbinning of the HETG data does not affect the results. The normalization of the HETG spectrum was allowed to differ by up to 10% from that of the ACIS-S data. A redshift of  $z = 1.0$  (taken from the most distant absorption system along the line of sight to the burst; Vreeswijk et al. 2000) was assumed throughout our analysis. The spectral fitting was performed using XSPEC v.11.0.1aj (Arnaud 1996), and all error bars quoted below are the 90% confidence limits for one interesting parameter.

The results of our spectral fitting analysis are summarized in Table 1. A power-law fit to the entire energy range (Fit #1) does not result in an adequate fit. Introducing intrinsic absorption (the Galactic column of  $2.1 \times 10^{21}$   $\text{cm}^{-2}$  is included in all fits) does not improve this result. The poor fit is a result of a line feature around 3.4 keV (observed frame) and of a significantly hardening of the data above  $\sim 5$  keV. This was noticed by Piro et al. (2000) who interpreted the excess above 5 keV as an iron recombination edge in emission. Ignoring this change of slope for the time being, we concentrate on fitting the data below 4.6 keV (the fits marked with a †). Fitting a power-law to this limited energy range still does not provide a good fit to the data (#3). Adding intrinsic absorption to the model (#4) only marginally helps the fit, with the added component only significant at the 92% level, according to the F-test. Replacing the absorber with a Gaussian emission line (Fit #5) does improve  $\chi^2$  substantially. The line is significant at the 98% level, and its centroid energy is tightly constrained around the energy of the He-like Fe  $K\alpha$

**Table 1.** Summary of fit results. A Galactic absorbing column of  $2.1 \times 10^{21} \text{ cm}^{-2}$  was included in all fits. In the table heading,  $N_{\text{H}}$  denotes the neutral hydrogen column density (units of  $10^{22} \text{ cm}^{-2}$ ) at the redshift of the source,  $E$  is the rest-frame centroid energy (in keV) of the Gaussian emission line,  $\sigma$  is the width of the line in keV, and ‘Sig.’ denotes the significance of the added model parameter as given by the F-test. PL=power-law, A=absorption, R=ionized reflection model & G=Gaussian.

Fit #	Model	$\Gamma_1$	$N_{\text{H}}$	$E$	$\sigma$	$\Gamma_2$	$\chi^2/\text{d.o.f.}$	Sig.	Notes
1	PL	$1.76^{+0.09}_{-0.10}$	–	–	–	–	99/60	–	–
2	A*PL	$1.83^{+0.14}_{-0.13}$	$0.24^{+0.40}_{-0.24}$	–	–	–	97/59	74%	–
3 <sup>†</sup>	PL	$1.83 \pm 0.11$	–	–	–	–	85/50	–	–
4 <sup>†</sup>	A*PL	$2.03^{+0.11}_{-0.19}$	$0.52^{+0.55}_{-0.40}$	–	–	–	80/49	92%	–
5 <sup>†</sup>	PL+G	$1.87 \pm 0.11$	–	$6.80^{+0.02}_{-0.19}$	0.01 <sup>fixed</sup>	–	72/48	98%	–
6 <sup>†</sup>	A*(PL+G)	$2.13^{+0.23}_{-0.21}$	$0.63^{+0.58}_{-0.43}$	$6.80^{+0.02}_{-0.19}$	0.01 <sup>fixed</sup>	–	65/47	97%	EW $\approx$ 300 eV
7 <sup>†</sup>	A*(PL+G)	$2.17^{+0.26}_{-0.21}$	$0.68^{+0.63}_{-0.44}$	$6.82^{+0.10}_{-0.11}$	$0.15^{+0.15}_{-0.11}$	–	62/46	84%	EW $\approx$ 400 eV
8	same as 6	–	–	–	–	–	96/57	–	–
9	A*(Bkn. PL+G)	$2.11^{+0.27}_{-0.19}$	$0.59^{+0.63}_{-0.40}$	$6.80^{+0.02}_{-0.19}$	0.01 <sup>fixed</sup>	$0.40^{+0.70}_{-0.84}$	72/55	–	$E_{\text{brk}} = 4.2 \pm 0.7 \text{ keV}$
10	A*(PL+R)	$2.61^{+0.59}_{-0.40}$	$1.37^{+0.84}_{-0.51}$	–	–	$0.0^{+0.44}_{-0.0p}$	76/56	–	$\log \xi = 3.01^{+0.07}_{-0.11}$

<sup>p</sup> Parameter pegged at lower-limit. <sup>†</sup> Ignored  $E > 4.6 \text{ keV}$ .

line<sup>1</sup>. Including intrinsic absorption in this model (Fit #6) improves the fit still further. Allowing the width of the Gaussian to vary (Fit #7) does not significantly improve the fit, but does show that the line is marginally resolved and is likely broadened. Therefore, the true error on the centroid energy is  $\pm 0.1 \text{ keV}$ , as the narrow line fit above missed a second minimum in  $\chi^2$  space at 6.9 keV. In summary, we can find an adequate fit to the data below 4.6 keV with a power-law plus Gaussian emission line model. The fit also seems to prefer absorption greater than that provided by the Galactic column, although this is significant only at the 97% confidence level.

Reintroducing the harder data, but leaving the model parameters the same as in Fit #6, greatly increases the  $\chi^2$  of the fit (#8). The residuals show that there is a clear change in slope at higher energies. Fitting the complete continuum with a broken power-law (#9) does a very good job in fitting the entire dataset, and implies that the observed spectrum may be a mixture of two separate emission features. Replacing the broken power-law model with a power-law plus Compton reflection spectrum (with incident power-law included) gives a very similar fit (#10; Fig. 2).

The photon-indices of the two power-laws are very different, with the Thomson-thick reflector subject to a very hard ( $\Gamma \approx 0$ ) ionizing continuum. The ionization parameter of the slab is well constrained, and, similar to the Gaussian line model, shows that emission from He-like iron is required with strong significance. However, the iron abundance and relative strength of the reflection features cannot be constrained with these data. The above result

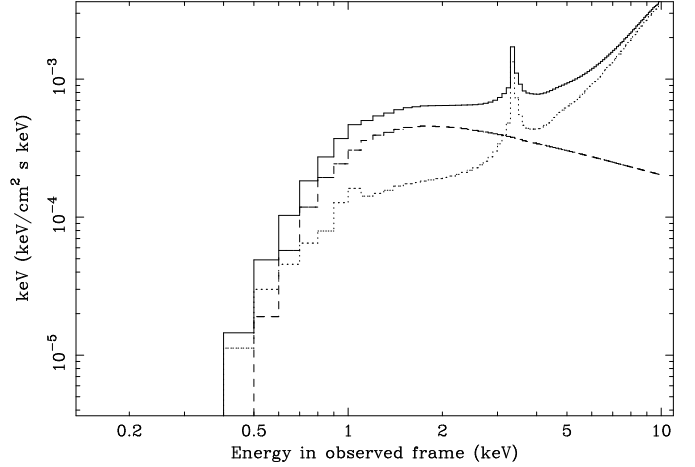


**Fig. 2.** Best fit model (#10) in physical units. The solid line show the total spectrum, while the dashed and dotted lines show the blast wave emission and reflected component, respectively.

was obtained assuming a solar abundance of iron and a reflection fraction of unity.

### 3. Discussion

In this paper we have, for the first time, fitted a physically sound model to the spectrum of the X-ray afterglow of a GRB that shows evidence of iron line emission. Our analysis applies to reflection from an optically thick, homogeneous medium, which seems to be required in order to explain the large equivalent width that is observed. The emission feature observed in the X-ray spectrum of GRB 991216 can be explained by reflection if identified with the recombination  $K\alpha$  line from He-like iron at 6.7 keV. Although there exists a significant zone of H-like Fe in the reflector, its  $K\alpha$  line is subject to resonant trapping and is ultimately destroyed by Thomson scat-

<sup>1</sup> However, if we ignore the change in continuum slope and fit a power-law plus Gaussian line model to the entire energy range, the upper-limit of the line energy is 6.98 keV at  $z = 1.02$  (roughly the error on the measured redshift). Therefore, we cannot strictly rule out a contribution from H-like iron.

tering. If, however, the emitting medium has a velocity dispersion of  $\sim 0.1c$  (Piro et al. 2000), resonant trapping would be suppressed (Lazzati et al. 2001), making the H-like line at 6.97 keV visible. On the other hand, the spectrum can be successfully modelled without kinematic line broadening since the observed width can be reproduced by Comptonization for an expansion velocity below the limit of  $0.1c$  inferred by Piro et al. (2000).

In order to fit the hardening of the spectrum above 5 keV (which was interpreted by Piro et al. (2000) as a recombination edge) we require the ionizing continuum to have a much harder power-law than the observed one. This hard continuum may result from the prompt or central engine emission and would be primarily responsible for ionizing the slab. The other, softer spectrum would then originate from the blast-wave emission, which at later times dominates most of the observed spectrum. If this power-law spectrum continues to  $h\nu \geq 511$  keV, a significant fraction of the energy in this early ionizing spectrum will be above the  $\gamma\gamma \rightarrow e^\pm$  formation energy threshold. This will cause new pairs to be formed in the originally optically thick scattering medium, an effect which amplifies the density of scattering charges and increases the temperature of the illuminating material. The effect of pair production on the line luminosity is twofold. On one hand, the electron density is increased, making the recombination time shorter and then the line more luminous. On the other hand, the Thomson opacity of the slab is increased, reducing the depth out of which line photons can escape without being scattered by free electrons. These two effects compensate and as a net result the line luminosity is slightly decreased by the increase of the electron temperature (Kallman et al. 2002). The results presented here are computed only up to an energy of 100 keV, so we do not take into account pair processes.

We find that iron enrichment is not necessary to reproduce the line strength, although if the true ionization parameter is substantially different than the best-fit value  $\xi \approx 10^3$ , then a moderately super-solar abundance will help bring the line to the required power (Ballantyne & Ramirez-Ruiz 2001; Ballantyne et al. 2002). In addition, even if at a non-statistically significant level, the model seems to underestimate the line strength in the grating spectrum, and a supersolar metallicity may cure this. Light elements such as S, Ar and Ca are not currently included in this reflection model (Ross & Fabian 1993), so it is not possible to determine if the small deviation at  $h\nu \sim 1.8$  keV is consistent with a S recombination edge.

The value of  $\xi \approx 10^3$  is predicted by the extreme clumping of ED models, but can also be accommodated in GD models if the reprocessing material is moderately clumped and/or the off-axis burst ionizing continuum is substantially dimmer than the observed burst emission. This is not unexpected, since the beaming break in GRB 991216 occurred quite early (1.5 days; see Halpern et al. 2000). Unfortunately, the statistical quality of the data does not allow clear conclusions to be drawn on the

line emission mechanism, and both GD and ED scenarios are consistent with the data.

In summary, our main conclusions are as follows. The iron line-like feature in the X-ray afterglow of GRB 991216 has properties consistent with reflection from an optically thick slab with solar metallicity and ionization parameter  $\xi \approx 10^3$ . The data constrain the energy of the line to be  $\approx 6.8$  keV, requiring recombination emission from He-like iron. There is some evidence for substantial intrinsic absorption at the source, consistent with the burst occurring within a gas-rich environment (such as a star-forming region). No kinematic broadening from an outflow is required by the data. The ionizing spectrum that impinges on the slab must however be harder than the afterglow spectrum that dominates the emission at  $h\nu < 4$  keV. All these findings can be accounted for by many of the emission mechanisms and geometries discussed in the literature. However, we have shown that ionized reflection models can describe the X-ray afterglow of GRB 991216, and that they may provide important information on the immediate environments of other bursts. Higher signal-to-noise data are required in order to have more insight in the properties and geometry of the line emitting material.

*Acknowledgements.* The authors thank the referee for his comments on the manuscript. DRB acknowledges financial support from the Commonwealth Scholarship and Fellowship Plan and the Natural Sciences and Engineering Council of Canada.

## References

- Antonelli L. A., Piro L., Vietri M., et al., 2000, *ApJ*, 545, L39  
 Arnaud K. A., 1996, *Astronomical Data Analysis Software and Systems V*, eds. Jacoby G. and Barnes J., p17, ASP Conf. Series volume 101.  
 Ballantyne D. R., Ramirez-Ruiz E., 2001, *ApJ*, 559, L83  
 Ballantyne D. R., Fabian A. C., Ross R. R., 2002, *MNRAS*, 329, L67  
 Böttcher M., Fryer C. L., 2001, *ApJ*, 547, 338  
 Halpern J., Uglesich R., Mirabal N., et al., 2000, *ApJ*, 543, 697  
 Kallman T., Mészáros P., Rees M. J., 2002, *ApJ* submitted (astro-ph/0110654)  
 Lazzati D., Campana S., Ghisellini G., 1999, *MNRAS*, 304, L31  
 Lazzati D., Ghisellini G., Amati L., Frontera F., Vietri M., Stella L., 2001, *ApJ*, 556, 471  
 Mészáros P., Rees M. J., 1998, *MNRAS*, 299, L10  
 Mészáros P., Rees M. J., 2001, *ApJ*, 556, L37  
 Piro L., Costa E., Feroci M., et al., 1999, *ApJ*, 514, L73  
 Piro L., Garmire G., Garcia M., et al., 2000, *Science*, 290, 955  
 Rees M. J., Mészáros P., 2000, *ApJ*, 545, L73  
 Ross R. R., Fabian A. C., 1993, *MNRAS*, 261, 74  
 Ross R. R., Fabian A. C., Young A. J., 1999, *MNRAS*, 306, 461  
 Vietri M., Stella L., 1998, *ApJ*, 507, L45  
 Vietri M., Ghisellini G., Lazzati D., Fiore F., Stella L., 2001, *ApJ*, 550, L43  
 Vreeswijk P. M., et al., 2000, *GCN Circ.* 496 (<http://gcn.gsfc.nasa.gov/gcn/gcn3/496.gcn3>)  
 Woosley S. E., 1993, *ApJ*, 405, 273  
 Woosley S. E., Weaver T. A., 1995, *ApJS*, 101, 181  
 Yoshida A., Namiki M., Yonetoku D., et al., 2001, *ApJ*, 557, L27